

An Improved PI Regulator Based Load Regulation in Constant Photovoltaic Power Supply System

A. Durgadevi¹, S. Arulsevi²

Department of Electronics and Instrumentation Engineering
Annamalai University, Chidambaram, Tamil Nadu, India.

Abstract

Due to scarcity of fossil fuel and increasing demand of power supply, we are forced to utilize the renewable energy resources. Considering easy availability and vast potential, world has turned to solar photovoltaic energy to meet its ever increasing energy requirement. In photovoltaic (PV) applications the grid tied systems often use a boost type converter to step up the output voltage to the utility level before the inverter stage. In grid connected PV systems due to load variation the output voltage may deviate from its nominal value. Hence, there is a need for closed loop control to regulate the output voltage and switching frequency of the PWM pulses are varied depends on the error.

In order to regulate the converter due to non linearity, conventional controller like PI controller is proposed and simulated. The performance of the PI controller is improved by including error limiter algorithm. The results reveal that the output voltage is regulated satisfactorily for increasing load current.

Keywords: — Photovoltaic, Pulse Width Modulation, Proportional Integral, Current Conduction Mode.

1. INTRODUCTION

Today photovoltaic (PV) systems are becoming more and more popular with increase of energy demand and there is also a great environmental pollution around the world due to fossils and oxides. In the grid connected PV power application, there are number of different topologies for DC-DC converters they are categorized into isolated and non-isolated topologies. The isolated topologies use a small-sized high frequency electrical isolation transformer, which provides the benefit of dc isolation between input and output, step or down of output voltage by changing the transformer turns ratio. They are very often used in switched mode dc power supplies. Popular topologies for a majority of applications are fly back, half-bridge and full bridge. In PV application the grid-tied systems often use these types of topologies, when electrical isolation is preferred for safety reasons.

Non isolated topologies do not have isolation transformer. They are almost always used in DC motor drives. These topologies are further categorized into two types: step down (buck) and step up (boost). The boost topology is used for stepping up the voltage. The grid-tied system uses a boost type converter to step up the output voltage to the utility level before the inverter stage. For a typical PV module the open

circuit voltage is about 21V and the MPP (Maximum Power Point) voltage is about 16V. And the utility grid voltage is 220V AC (110V AC).

Therefore, enough high voltage amplification is obligatory to realize the grid connected function. Thus, the solar module with boost converter can stabilize the output voltage and slightly increase the overall efficiency [1]. The schematic of the PV module with boost converter is shown in fig.1. Hence, an attempt is made in this paper to study the output voltage regulation due to load change by connecting the PV module with boost converter. All the simulation works are carried out using MATLAB/Simulink software.

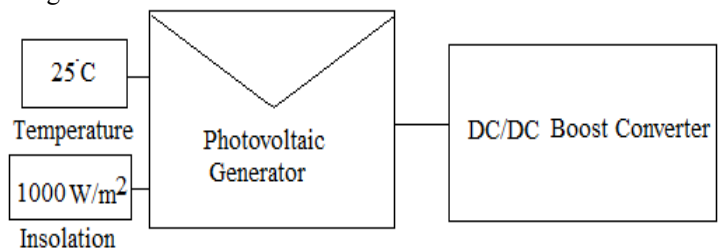


Fig.1. Photovoltaic module with DC-DC boost converter.

2. Mathematical modeling of photovoltaic cell

A photovoltaic module consists of a number of interconnected solar cells encapsulated into a single unit [2]. In order to predict the power extracted from the solar modules and the module current-voltage (I-V) characteristics, it is important to model the solar cell. Once the I-V characteristics of a single solar cell are determined using the model, one must then expand that model to determine the behavior of a PV array or module. A Photovoltaic array comprises many solar cells wired in series and in parallel.

A solar cell model is shown in Fig.2. The model, takes into account the variation of the photoelectric current, when the radiation and the temperature changes, and also the variation of the diode saturation current when the temperature changes. In this, the current generator I_L represents the generated photoelectric current while the diode (D_1) and the resistance R_s , which takes into account the internal electrical losses of the photovoltaic module [3].

By applying the Kirchhoff law to the node of the circuit reported in Fig. 1, the current 'I' produced by the photovoltaic module is obtained as

$$I = I_L - I_D \quad (1)$$

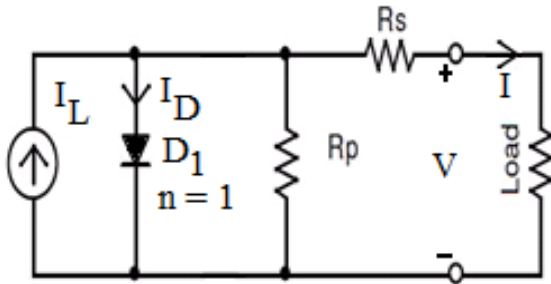


Fig.2. Equivalent circuit of photoelectric module.

The I_D diode current is given by the Shockley equation:

$$I_D = I_o \left[\exp \left(\frac{q(V+IR_s)}{\gamma k T_c} \right) - 1 \right] \quad (2)$$

where $-I_D$ is the diode current; I_L is the photoelectric current related to a given condition of radiation and temperature; V is the output voltage [V]; I_o is the saturation diode current [A]; γ is the form factor which represents an index of the cell failing; R_s is the series resistance of the cell [Ω]; q is the electric charge ($1.602 \times 10^{-19} \text{C}$); k is the Boltzmann's constant ($1.381 \times 10^{-23} \text{K}$); T_c is the module temperature [K].

By substituting (2) in (1), the following equation is obtained, which represents the I-V module characteristics curve under generic radiation and temperature conditions.

$$I = I_L - I_o \left[\exp \left(\frac{q(V+IR_s)}{\gamma k T_c} \right) - 1 \right] \quad (3)$$

The model proposed in equation no. (3) describes the working of a photovoltaic module under the hypothesis of knowing the values of γ , R_s , I_o and I_L . In order to take into account the variation of the diode saturation current and the photoelectric current when temperature and radiation change, with respect to standard conditions, the model is completed with the following equations:

$$I_o = I_{o,REF} \left(\frac{T_c}{T_{c,REF}} \right)^3 \exp \left[\left(\frac{q E_g}{k \gamma} \right) \left(\frac{1}{T_{c,REF}} - \frac{1}{T_c} \right) \right] \quad (4)$$

$$I_L = \left(\frac{G}{G_{REF}} \right) [I_{L,REF} + \mu_{ISC} (T_c - T_{c,REF})] \quad (5)$$

where E_g is the energy gap of the material with which the cell is made (for the silicon it is 1.12 eV); G is the radiation [W/m^2]; G_{REF} is the radiation under standard conditions [W/m^2]; $I_{L,REF}$ is the photoelectric current under standard conditions [A]; $T_{c,REF}$ is the module temperature under standard conditions [K]; μ_{ISC} is the temperature coefficient of the short circuit current [A/K], given by the manufacturer according to CEI EN 60891 standard [4].

The cell junction temperature T_j is a function of the ambient temperature and the solar radiation. It is the operating temperature of the PV cells and is assumed to be uniform in the whole PV collector. T_j can be expressed as follows:

$$T_j = T + k_1 G \quad (6)$$

G - Global horizontal irradiation in W/m^2 , T -ambient temperature ($^{\circ}\text{C}$), T_j -cell junction temperature ($^{\circ}\text{C}$).

3. Simulation Results for I-V and P-V characteristics with varying Temperature and Insolation Levels in Matlab-Simulink Environment

The solar cell I-V characteristics represented by one diode mode as given in equation (3) is implemented in Matlab / masked Simulink environment as shown in Fig. 3 and the simulated results are presented and discussed. The inputs to the system are ambient temperature T_{aC} and radiation G while the output are array voltage V_{pv} and array current I_{pv} [5].

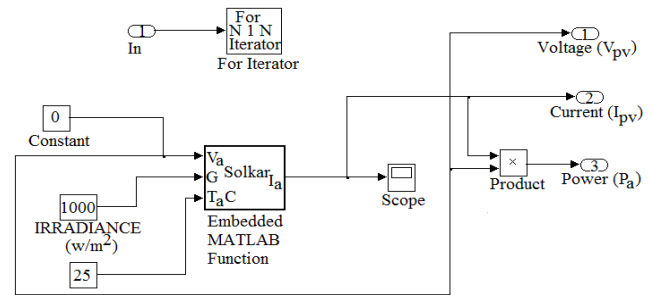


Fig.3. Masked-simulink model of Photovoltaic array.

3.1 Simulation Results

A single PV cell produces an output voltage less than 1V, about 0.6V for crystalline silicon (Si) cells, thus a number of PV cells are connected in series to achieve a desired output voltage. When series-connected cells are placed in a frame, it is called as a module. Most of the commercially available PV modules with crystalline-Silicon cells have either 36 or 72 series-connected cells.

A 36-cell module provides a voltage suitable for charging a 12V battery, and similarly a 72-cell module is appropriate for a 24V battery. This is because most of PV systems used to have back up batteries, however today many PV systems do not use batteries for example, grid-tide systems. Furthermore, the advent of high efficiency DC-DC converters has alleviated the need for modules with specific voltages.

When the PV cells are wired together in series, the current is the same as the single, but the voltage output is the sum of each cell voltage. The simulated I-V characteristics for different cells (3-72 numbers) are shown in Fig. 4(a).

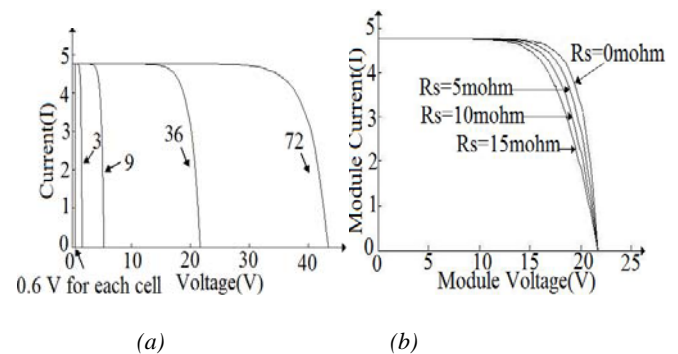


Fig.4. Simulated (a) I-V characteristics for different Photovoltaic cells, (b) Effect of series resistance on I-V characteristics.

The series resistance (R_s) of the Photovoltaic module has a large impact on the slope of the I-V curve near the open-circuit voltage (V_{oc}) [4]. This can be seen from simulated result as shown in Fig. 4(b). Hence the value of R_s is calculated by evaluating the slope dv/di of the curve at the V_{oc} as 5.0 milli ohms.

In this work, 36-cell module connected in series is considered. The manufacturer parameters of the Photovoltaic module are tabulated in Table I.

Table I: Standard Test Condition data

<i>Electrical characteristics</i>	
Cell	Poly-crystalline silicon
No of cells and connections	36 in series
Open circuit Voltage (V_{oc})	21.75 V
Short – circuit current (I_{sc})	4.75A
Maximum Power Voltage at P_{max} (V_{nm})	17.25 V
Maximum Power Current (I_{nm})	4.515 A
Maximum Power (P_{max})	77.88 W (+10%/-5%)
Module Efficiency (η_m)	13%
Series Fuse Rating	10 A
Type of output terminal	Junction Box
Temperature coefficient of I_{sc}	$0.65e-3 \pm 0.015\%/^{\circ}C$
Temperature coefficient of V_{oc}	$-160 \pm 20mV\%/^{\circ}C$
Temperature coefficient of Power	$-0.5 \pm 0.05\%/^{\circ}C$

3.2 Solar I-V Characteristics By Varying Insolation Levels and Temperature

The results of the simulation of the PV array (36-cells) in SIMULINK are shown in Fig. 5 and 6. Fig. 5(a) shows the simulated I-V curve for 25°C and Fig. 5(b) represents the P-V characteristics of the PV array for irradiation level of 1000w/m2. It is seen from Fig. 5(a) that the maximum power point is located at the knee of the I-V curve.

At this Maximum Power Point (MPP), the solar array is matched to its load and when operated at this point the array will yield the maximum power output. From Fig. 5(b), it is observed that the power output has an almost linear relationship with array voltage unit, hence the MPP is attained. Any further increase in voltage results in power reduction [5].

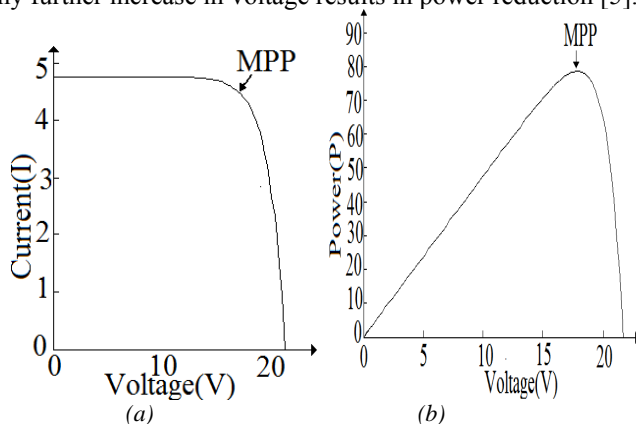


Fig.5. PV array simulated curves (a) I-V curve (25°C) and (b) P-V curve (1000w/m2).

It can be observed from simulated results as shown in Fig. 6(a), the photo current is directly proportional to irradiation. It is noted from Fig. 6(b) that the terminal voltage increases with decreasing temperature.

This effect is due to the band gap energy of semiconductor materials, which reduces with decrease in temperature resulting in more electrons making it to the conduction band and hence a more efficient solar cell is achieved.

It can be observed from simulated results as shown in Fig. 6(a), the power output is directly proportional to irradiation. As such, smaller decrease in irradiation will result in reduced power output from the solar panel.

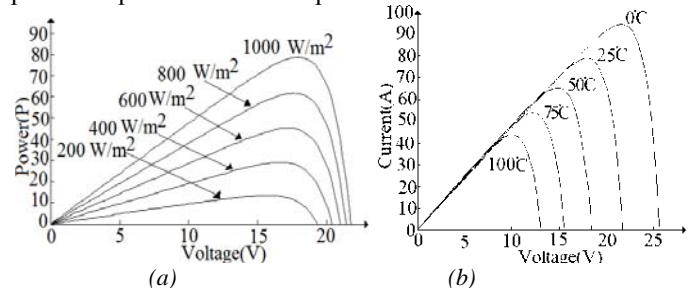


Fig.6. Simulated waveforms showing the effect of (a) radiation and (b) temperature on P-V characteristics.

The manufacturers data at standard conditions are given as $P_{max} = 80W$, $I_{max} = 4.515 A$ and $V_{max} = 21.6V$. The simulation results obtained were: $P_{max} = 78.51W$, $I_{max} = 4.515 A$ and $V_{max} = 21.65V$. It is seen that the simulation model showed excellent correspondence to manufacturer’s data and therefore this model was considered sufficient for the purpose of further study [4&8].

It is noted from Fig. 6(b) that the terminal voltage increases with decreasing temperature, thereby reducing the power. The simulated P-V characteristics showing the effect of irradiation and temperatures are shown in Fig.6 (a) & (b).

4. Designing of Boost converter

4.1 Circuit diagram of boost converter.

Fig. (7) shows the schematic diagram of boost converter, which consists of DC supply voltage V_s , boost inductor L , controlled switch S , diode D filter capacitor C and load resistance R . The current and voltage waveforms of the converter in CCM are presented in fig.8.

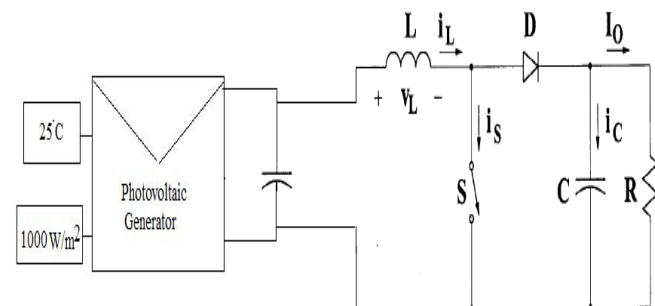


Fig.7. Circuit diagram of boost converter with PV module.

When the switch S is on and diode D is off current in the boost inductor increases linearly and when the switch S is turned off, energy stored in the inductor is released through the diode to the output RC circuit using faradays law for the boost inductor as given in (7).

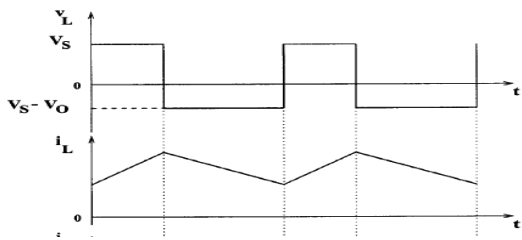


Fig.8. Theoretical voltage and current waveforms of boost converter.

$$V_s DT = (V_o - V_s)(1 - D)T \quad (7)$$

The DC voltage transfer function turns out to be,

$$M_v = \frac{V_o}{V_s} = \frac{1}{(1-D)} \quad (8)$$

As the name of the converter suggest that the output voltage is always greater than the input voltage. The boost converter operates in the CCM for $L > L_b$. The calculated value of inductance $L = 23.5628 \mu H$.

To limit the ripples in the output side, larger filter capacitor is required. The filter capacitor must provide the output dc current to the load when diode D is off. The minimum value of filter capacitance calculated that results in the voltage ripple V_r is given by $C_{min} = 13.0714 \mu F$.

Thus the boost converter is designed in the open loop for the supply voltage of 21.7V DC, which is generated by the Photovoltaic panel.

Fig.9 shows the simulated voltage and current waveforms of boost converter. It is seen that these waveforms are agreed closely with theoretical waveforms as shown in fig.8.

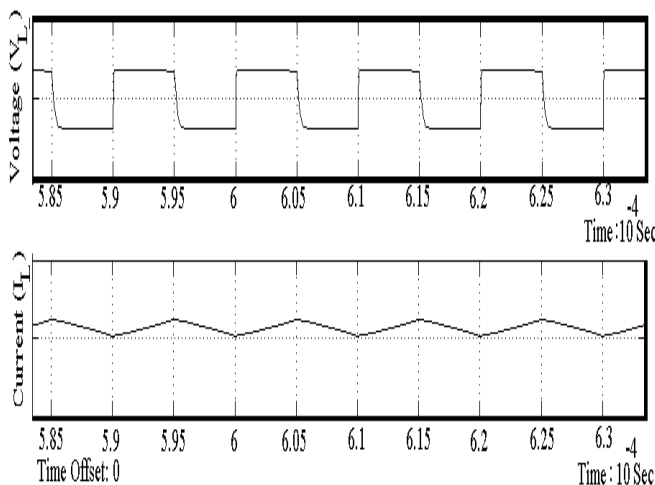


Fig.9. Simulated waveforms showing the voltage and current of boost converter.

It is observed from the fig.10 that in open loop operation, the converter output deviates from the required output voltage 40 and settles at new value after a sudden load current changes at time $t = 0.0512$ sec from 0.77A to 1.053A. Hence, a closed loop control is needed to regulate the output voltage against load variation [9].

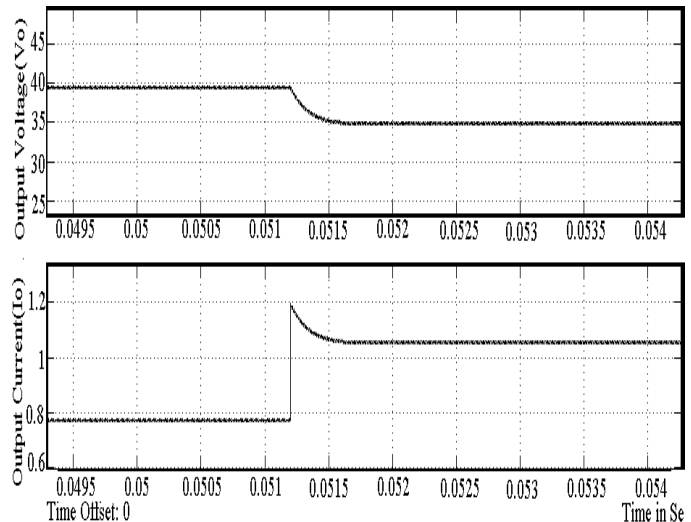


Fig.10. Output voltage (V_o) and current (I_o) for sudden load current variation of 0.77A to 1.053A.

5. closed loop simulation

The block diagram of closed loop simulation is shown in fig.11. to regulate the output voltage V_o , the switching frequency of the PWM pulses are varied depends on error. Since, output voltage (V_o) is very sensitive to load variation by producing large deviation from nominal value for small variation in load. Hence, a closed loop control is designed to maintain tight regulation of V_o , against load variation.

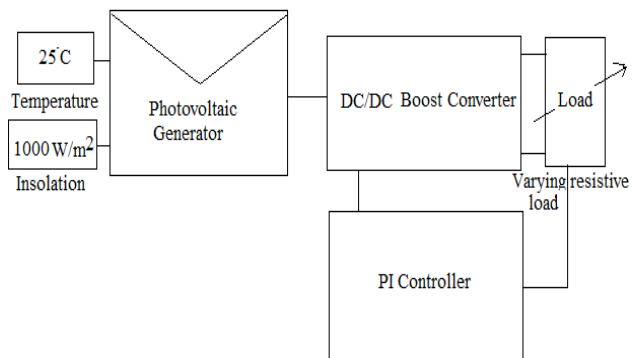


Fig.11. Block diagram of closed loop controlled boost converter for solar installation.

5.1 Closed –loop control using PI controller with error

Limiter algorithm

The conventional PI controller parameters are obtained by Z-N open loop method [9] as proportional gain $K_c = 0.81$ and integral gain $K_i = 1.333$. Regulated output voltage for sudden decrease in load current (I_o) at time $t = 0.0512$ sec from 0.77A to 1.053A is shown in fig.12. From fig.12 it is observed that the falling edge of the regulated output voltage is slightly increased due to sudden load variation. To suppress this slight variation, regulate the output voltage at reference voltage and to improve the overall performance of the regulator circuit, an error limiter algorithm is included in PI controller based regulator circuit.

Hence, the overall performance of the PI controller is increased. The regulated output voltage settles at reference voltage without ripples which is shown in fig.13.

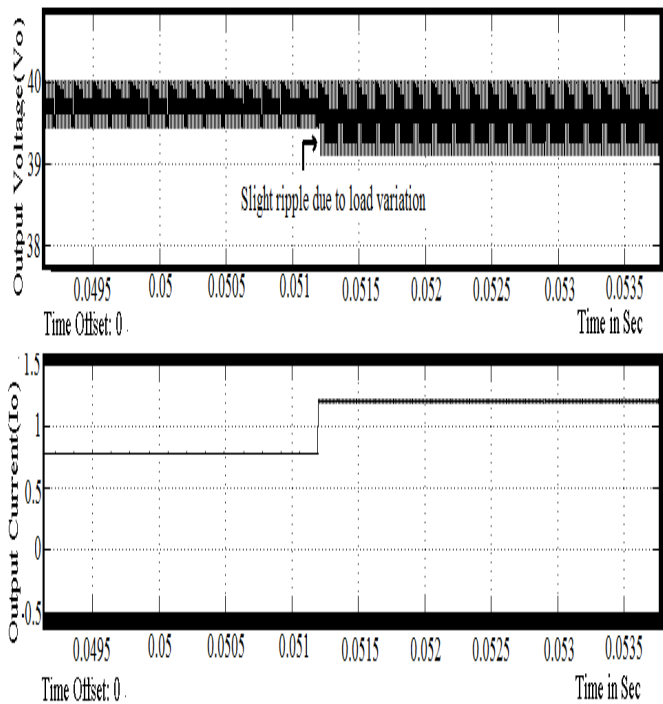


Fig.12. Output voltage (V_o) and current (I_o) for sudden load current variation of 0.77A to 1.053A with slight increased ripple in falling edge of output voltage (V_o).

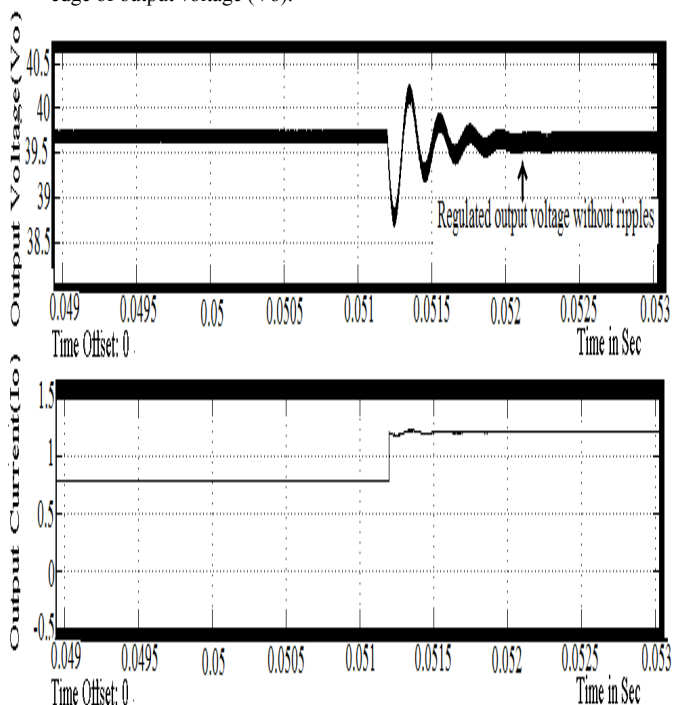


Fig.13. Output voltage (V_o) and current (I_o) for sudden load current variation of 0.77A to 1.053A with error limiter algorithm based PI Controller.

From the simulation results of fig.13 it is observed that the output voltage (V_o) is well regulated and maintained at reference voltage 40V with negligible offset. The performance of PI controller is given in Table II.

TABLE II
 PERFORMANCE MEASURES

R_o	V_o		I_o	
	Calculated	Simulated	Calculated	Simulated
51 Ω	40V	39.3V	0.784A	0.77A
33 Ω	35V	34.99V	1.06A	1.053A
PI Controller				
R_o (Down load)	V_o (Regulated without error limiter)	V_o (Regulated with error limiter)	I_o (Down load)	
51 to 33 Ω	39.375V	39.5	0.77 to 1.053A	
Improved Regulation (V)		0.125V		
Over all Offset (V)		0.5V		

6. Conclusion

This paper presented the simulation of open loop and closed loop controlled boost converter system for solar installation system. Matlab models for open loop and closed loop systems are developed using the blocks of Simulink and the same are used for simulation studies.

The closed loop system is able to maintain constant voltage. It has been proved that addition of error limiter algorithm solves some of the slight variation in regulated output voltage which has appeared previously and enhanced the performance of regulator circuit notably. This converter has the advantages like reduced hardware and good output voltage regulation. It can be concluded that PI controller is capable of regulating required constant voltage due to load variation.

REFERENCES

- [1] S. A. Zabalawi, G. Mandic and A. Nasiri, "Utilizing energy storage with PV for residential and commercial use," Industrial Electronics, 2008. IECON 2008. 34th Annual Conference of IEEE, pp. 1045-1050, 10-13Nov. 2008.
- [2] Akihiro Oi, "Design and Simulation of Photovoltaic Water Pumping System", Master of Science Thesis, California Polytechnic State University, 2005.
- [3] E. Koutroulis, K.Kalaitzakis and N.C.Voulgaris., "Development of a microcontroller-based, photovoltaic maximum power point tracking control system", IEEE Trans. Power Electronics, vol. 16, pp. 46-54, Jan. 2001.
- [4] C. Hua and C. Shen, "Study of maximum power tracking techniques and control of dc-dc converters for photovoltaic power system," in Proc. 29th Annu. IEEE PESC May 17-22, 1998, vol. 1, pp. 86-93.
- [5] J. A. Gow, C. D. Manning "Development of a photovoltaic array model for use in powerelectronics simulation studies," IEE Proceedings on Electric Power Applications, vol. 146, no. 2, pp. 193-200, March 1999.
- [6] D. Sera, R. Teodorescu, P. Rodriguez. "PV Panel Model Based onDatasheet Values", IEEE International Symposium on Industrial Electronics, pp. 2392-2396, June 2007.
- [7] M.F. Schonardie, D.C. Martins. "Solar Grid-Connected Three-PhaseSystem With Active And Reactive Power Control And Input Voltage Clamped" 14th IEEE International Conference on Electronics, Circuits and Systems, pp. 463-466 Dec. 2007.
- [8] D. Chan and J. Phang. "Analytical Methods for the Extraction of Solar-Cell Single- and Double-Diode Model Parameters from I-V Characteristics" IEEE Transactions on Electron Devices, pp. 286-293, 1987.
- [9] A. Durgadevi, "Design of intelligent controller for quasi resonant converters", M.E. dissertation, Annamalai Univ., Chidambaram, 2008.